JOURNAL OF BACTERIOLOGY, Sept. 2003, p. 5398–5407 Vol. 185, No. 18
0021-9193/03/$08.00+0 DOI: 10.1128/JB.185.18.5398–5407.2003

Extracellular Polysaccharides Associated with Thin Aggregative Fimbriae of *Salmonella enterica* Serovar Enteritidis

A. P. White,[1,2] D. L. Gibson,[1] S. K. Collinson,[1] P. A. Banser,[1] and W. W. Kay[1]*

Department of Biochemistry and Microbiology, University of Victoria, Victoria, British Columbia V8W 3P6,[1] *and Department of Microbiology and Infectious Diseases, University of Calgary, Calgary, Alberta T2N 4N1,*[2] *Canada*

Received 26 February 2003/Accepted 25 June 2003

Lipopolysaccharide (LPS) O polysaccharide was identified as the principle factor impeding intercellular formation of intact thin aggregative fimbriae (Tafi) in *Salmonella enterica* serovar Enteritidis. The extracellular nucleation-precipitation assembly pathway for these organelles was investigated by quantifying fimbrial formation between Δ*agfA* (AgfA recipient) and Δ*agfB* (AgfA donor) cells harboring mutations in LPS (*galE*::Tn*10*) and/or cellulose (Δ*bcsA*) synthesis. Intercellular complementation could be detected between Δ*agfA* and Δ*agfB* strains only when both possessed the *galE* mutation. LPS O polysaccharide appears to be an impenetrable barrier to AgfA assembly between cells but not within individual cells. The presence of cellulose did not restrict Tafi formation between cells. Transmission electron microscopy of w^+ *S. enterica* serovar Enteritidis 3b cells revealed diffuse Tafi networks without discernible fine structure. In the absence of cellulose, however, individual Tafi fibers were clearly visible, appeared to be occasionally branched, and showed the generally distinctive appearance described for *Escherichia coli* K-12 curli. A third extracellular matrix component closely associated with cellulose and Tafi was detected on Western blots by using immune serum raised to whole, purified Tafi aggregates. Cellulose was required to tightly link this material to cells. Antigenically similar material was also detected in *S. enterica* serovar Typhimurium and one diarrheagenic *E. coli* isolate. Preliminary analysis indicated that this material represented an anionic, extracellular polysaccharide that was distinct from colanic acid. Therefore, Tafi in their native state appear to exist as a complex with cellulose and at least one other component.

Thin aggregative fimbriae (Tafi) (formerly SEF17) are produced by most *Salmonella* strains and isolates of *Escherichia coli*, in which these organelles have been termed curli. In *Salmonella*, the divergently transcribed *agfDEFG* and *agfBAC* operons are required for production of functional Tafi (10, 35). Tafi are comprised primarily of AgfA subunits, and thus far there is evidence for the presence of only one other protein in the fiber, AgfB (7, 46). Tafi and curli fibers are remarkably stable, requiring treatment with 90% formic acid to depolymerize (3, 12). These fibers bind the hydrophobic dye Congo red (CR) (13), presumably due to the similar β-strand structures of AgfA and AgfB (31, 46).

AgfA and AgfB are interesting sequence homologues that are likely the result of several gene duplications; they are nearly identical in size and share many structural features. Despite their similarities, they have very different biochemical properties (46). Both proteins are required for fimbrial polymerization, with AgfA substantially predominating in the fimbriae. AgfEFG proteins participate in fiber formation and somehow ensure the fidelity of assembly. Deletion of *agfE* or *agfF* leads to the production of fimbriae with altered biochemical properties (9), whereas deletion of *agfG* disrupts fimbrial formation altogether (28). AgfD is a positive transcriptional regulator of the *agf* operon (19) and is required for Tafi biosynthesis (36).

* Corresponding author. Mailing address: Department of Biochemistry and Microbiology, University of Victoria, Victoria, British Columbia V8W 3P6, Canada. Phone: (250) 721-7078. Fax: (250) 721-8855. E-mail: wkay@uvic.ca.

There is growing interest in the relationship between Tafi (or curli) production in *Salmonella* (or *E. coli*) and the formation of biofilms (4, 24, 32, 39). Tafi (curli) production by many *S. enterica* and *E. coli* strains is tightly regulated by growth conditions, normally occurring at temperatures below 30°C (17, 37). In *Salmonella enterica* serovar Enteritidis 3b, Tafi are produced under less stringent conditions at both 28 and 37°C (12). These differences in regulation are likely due to differences in the *agfD* promoter sequence (37, 44). Recently, AgfD was shown to regulate production of another extracellular substance, cellulose (36, 48). Tafi and cellulose form a highly resistant extracellular matrix which may be important for ensuring bacterial survival in harsh environments (39). Capsular polysaccharides, such as colanic acid (CA), have also been implicated in the formation of Tafi- and curli-associated biofilms (33). These substances appear to be important for maintenance of space between cells and development of complex three-dimensional architectures (14).

Assembly of Tafi or curli fibers has been proposed to occur extracellularly, perhaps in the midst of other components. The current assembly hypothesis allows for fimbrial growth by addition of subunits principally to the distal end of the growing fibers (20). This is unique among fimbriae and has been termed the extracellular nucleation-precipitation pathway (40). The hypothesis is based upon the intercellular complementation of an *E. coli* MC4100 *csgA* mutant grown in close proximity to a *csgB* mutant (CsgA donor) on solid medium (20). Complementation yielded cells which possessed assembled curli and as a result were able to bind the dye CR. However, these experiments could not be reproduced in *S. enterica* serovar Enteri-

tidis 3b with precisely defined *agfA* and *agfB* mutant strains (46). For this study we devised an intercellular complementation strategy applicable to enteric strains more native than *E. coli* MC4100.

S. enterica serovar Enteritidis 3b possesses smooth lipopolysaccharide (LPS) O polysaccharide and produces cellulose in concert with Tafi (48). In contrast, *E. coli* MC4100 produces neither LPS O polysaccharide (27) nor cellulose (48). To allow for these differences, *S. enterica* serovar Enteritidis 3b Δ*agfA* and Δ*agfB* strains were rendered LPS O-polysaccharide deficient by introducing a *galE*::Tn*10* mutation and cellulose deficient by deleting *bcsA*, coding for cellulose synthase (34). Intercellular complementation between strains did not readily occur and did so only when the donor and acceptor were LPS O-polysaccharide deficient. Thus, LPS O polysaccharide substantially interferes with Tafi formation between cells under normal conditions, indicating that Tafi assembly does not normally occur intercellularly. Additional experiments with Δ*bcsA* strains revealed that Tafi in their native state exist as a complex with cellulose and at least one other extracellular polysaccharide (EPS).

MATERIALS AND METHODS

Bacterial strains, media, and growth conditions. *S. enterica* serovar Enteritidis 27655 strain 3b and its Δ*wcaJ* mutant, *S. enterica* serovar Typhimurium SL7207 (22), and *E. coli* Vietnam I/1 (13) were routinely grown in T broth (12) at 28 or 37°C for 24 or 48 h, with shaking at 200 rpm, or on T agar (T) or T agar plus CR (100 μg/ml) indicator plates (TCR agar) as previously described (11).

Generation of Δ*bcsA* and Δ*wcaJ* strains. An in-frame deletion removing 1,998 bp in *bcsA* (encoding amino acids 165 to 828 in BcsA) was generated as previously described (48) with some modifications. Primer YHJ05 was modified to contain an *Eco*RI site instead of a *Bam*HI site, and a new YHJ07 primer (CCACTGCAGATTCGCGCCGCCTTCAGTAA [a *Pst*I site is underlined]) was generated since *S. enterica* serovar Typhimurium *bcsA* contains a unique *Eco*RI site corresponding to amino acids 828 to 829; primers YHJ06 and YHJ08 were used as described previously (48). An in-frame deletion removing amino 1,206 bp in *wcaJ* (encoding amino acids 34 to 436 in WaaJ) was generated similarly by using PCR primers *wcaJ*01 (GGTGAATTCAAAAACCGGGC ACGC [an *Eco*RI site is underlined]), *wcaJ*02 (GAACTGCAGCCCGCCA AACA [a *Pst*I site is underlined]), *wcaJ*03 (GACCTGCAGTAAATCCGCGA [a *Pst*I site is underlined]), and *wcaJ*04 (GTAAAGCTTGGTCAGCTCCA [a *Hin*dIII site is underlined]). For each construct, the two PCR fragments generated were directionally cloned into *Eco*RI-*Hin*dIII-cut pTZ18R (Amersham Biosciences) and subcloned into pHSG415 (21). The Δ*bcsA* or Δ*wcaJ* mutation was introduced into the chromosomes of *S. enterica* serovar Enteritidis strains according to procedures described previously (47) with modifications: Ap^r plasmid-cointegrate colonies were selected after growth for 18 h at 42°C, and Ap^s Δ*bcsA* mutants were selected after two or three 18-h passages at 28°C. Mutants were identified by PCR screening with primers *bcsA*ko1 (CGGCCCGTTACCTCAT TCAG), *bcsA*ko2 (TTCAGCACCGCTTTCGACGC), *bcsA*wt1 (CAGAAACG AGCGTGTCGGCA), *wcaJ*ko1 (CGCTGCTGAATCAGTAACGT), *wcaJ*ko2 (TT AGCGCCGCTGATCGTTTT), and *wcaJ*wt1 (GCGACGCCAGCACGATAT CT), based on the *S. enterica* serovar Typhimurium DNA sequences (GenBank accession numbers AJ315770 and AF285085).

Generation of *galE*::Tn*10* mutants of *S. enterica* serovar Enteritidis 3b Δ*agfA* and Δ*agfB* strains. Phage stocks prepared after growth of transducing phage P22 *int3* HT 12/4 on *S. enterica* serovar Typhimurium LT2-TN1117 were used to infect *S. enterica* serovar Enteritidis 3b, Δ*agfA*, and Δ*agfB* cells at multiplicities of infection ranging from 0.01 to 5. Transductants were selected on Luria-Bertani plates containing tetracycline (16 μg/ml) and were rendered phage free by passage on Green plates (8). Potential *galE*::Tn*10* transductants were screened with indicator plates specific for galactose fermentation (23). *galE* phenotypes were confirmed by the absence of LPS O polysaccharide (O antigen) after growth on nutrient agar without galactose (23). *galE*::Tn*10* mutants grown on T agar (see Fig. 1 to 3) were severely depleted in O antigen as judged by sodium dodecyl sulfate-polyacrylamide gel electrophoresis (SDS-PAGE) and LPS-silver staining, but trace amounts (<10% of wild-type [w^+] levels) were detected.

Purification of Tafi from *S. enterica* serovar Enteritidis Δ*bcsA galE*::Tn*10*. Fimbriae were isolated and purified from plate-grown cells as previously described (12). SDS-PAGE sample buffer-insoluble material which did not enter the stacking gel was recovered, washed three times in distilled water (dH_2O), and lyophilized. This material was resuspended in dH_2O and treated with 90% formic acid before SDS-PAGE and Western blotting.

Intercellular complementation. *S. enterica* serovar Enteritidis 3b and the Δ*agfA*, Δ*agfB*, and related mutants were grown overnight at 28°C in T broth; cultures were normalized to an optical density at 600 nm (OD_{600}) of 1, and sterile swabs were used to streak different Δ*agfA* and Δ*agfB* combinations immediately adjacent to each other on TCR agar. Any differences in colony color due to variable CR binding were recorded after growth for 24 or 48 h at 37°C. For coplating experiments, 500-μl portions (OD_{600} of 0.5) of two different Δ*agfA* and Δ*agfB* cultures were combined, and a 100-μl aliquot was plated onto TCR agar. For each control strain, 100 μl of the original cell suspension at an OD_{600} of 1 was plated directly. Following growth for 24 h at 37°C, cells were scraped off the agar and resuspended in 1 ml of 10 mM Tris (pH 7.2). For SDS-PAGE and immunoblotting, cell samples at an OD_{600} of 4 were aliquoted, buffer was removed, and cells were treated as described below. For the CR binding assay (45), cells were normalized to an OD_{600} of 10 per ml and left to equilibrate for 1 h at room temperature (RT). After removal of cells by centrifugation, the amount of CR released into the buffer was determined by measuring the absorbance at 480 nm.

SDS-PAGE and Western blot analyses. Cell pellets from 4 OD_{600} units of cells were resuspended in 100 μl of SDS-PAGE sample buffer (26) and boiled for 10 min, and cellular debris was pelleted by centrifugation (15,600 × *g*, 5 min). These samples were washed with 500 μl of dH_2O, resuspended in 250 μl of 90% formic acid, frozen, and lyophilized. For analysis of proteins secreted into the agar, cells were removed and plugs of ~8 mm in diameter were taken (9), resuspended in 500 μl of dH_2O or 98% formic acid, frozen, and lyophilized. Samples were resuspended in SDS-PAGE sample buffer before separation by SDS-PAGE (26). Proteins and other materials were electrophoretically transferred to nitrocellulose in a glycine (192 mM)-Tris (25 mM, pH 8.3)-methanol (20%) solution by using a Mini-Protean II apparatus (Bio-Rad Laboratories). Proteins and associated material were detected by using immune serum raised to purified whole Tafi followed by goat anti-rabbit immunoglobulin G–alkaline phosphatase secondary antibody (Cedarlane Laboratories Ltd.) and nitroblue tetrazolium and BCIP (5-bromo-4-chloro-3-indolylphosphate) substrates (12).

Electron microscopy. *S. enterica* serovar Enteritidis 3b strains grown on T agar were resuspended in 10 mM Tris (pH 8) and deposited on 0.5% Formvar-coated nickel grids. The immunogold labeling procedure was as follows: 40 min at RT in 1% bovine serum albumin–0.15% NaCl–10 mM Tris (pH 8), 45 min at RT with AgfA-specific monoclonal antibody ascites 3A-12 diluted 1:1,000 in 0.1% bovine serum albumin–Tris–NaCl (diluent), and 30 min at RT with goat anti-mouse immunoglobulin G–10-nm-diameter gold (Cedarlane Laboratories Inc.) diluted 1:20 in diluent. Washes between steps were performed with Tris-NaCl. For negative staining only, cells were deposited on 0.5% Formvar-coated copper grids, rinsed in dH_2O, and stained with 1 to 2% uranyl acetate (pH 7). All samples were visualized with a Hitachi H7600 transmission electron microscope under HC-zoom mode at 100 kV.

RESULTS

Morphological characterization of *S. enterica* serovar Enteritidis Δ*bcsA* and *galE* mutants. Strains with Δ*bcsA* and/or *galE*::Tn*10* mutations were generated from *S. enterica* serovar Enteritidis 3b or the Δ*agfA* or Δ*agfB* mutant. The phenotypes of these strains were compared after growth on TCR agar (Table 1). All *agfBA*$^+$ strains exhibited an aggregative colony morphology and high CR binding, whereas all Δ*agfA* or Δ*agfB* strains were nonaggregative, with a much lower CR binding (Table 1). Introduction of the *bcs*A deletion caused a color change in all strains and a slight drop in CR binding in Δ*agfA* or Δ*agfB* strains (Table 1). These phenotypes matched those recently reported for similar Δ*bcsA* strains of *S. enterica* serovar Typhimurium (48). Introduction of the *galE* mutation resulted in different effects. In *agfBA*$^+$ strains a drop in aggregative morphology was observed, but minimal changes in CR binding were measured (Table 1). In Δ*agfA* or Δ*agfB* strains, a

TABLE 1. Morphological characterization of *S. enterica* serovar enteritidis 3b and isogenic *agfA* or *agfB* mutants

Strain[a]	Colony color[b]	Morphology[c]	*S. enterica* serovar Typhimurium morphology[d]	CR bound (μg)[e]
3b (*agfBA*$^+$)	Red	Ag(++)	rdar	35.8 ± 9.9
Δ*bcsA*	Red-brown	Ag(++)	bdar	44.1 ± 12.3
galE::Tn*10*	Orange-brown	Ag(+)	N/A[f]	34.7 ± 6.1
Δ*bcsA galE*::Tn*10*	Orange-brown	Ag(+)	N/A	34.5 ± 2.9
Δ*agfA* mutant	Pink	NAg	pdar	5.6 ± 0.6
Δ*bcsA*	White	NAg	saw	3.7 ± 0.4
galE::Tn*10*	Pink-orange	NAg	N/A	8.4 ± 1.5
Δ*bcsA galE*::Tn*10*	Pink	NAg	N/A	7.3 ± 1.5
Δ*agfB* mutant	Pink	NAg	pdar	4.6 ± 0.6
Δ*bcsA*	White	NAg	saw	3.6 ± 0.6
galE::Tn*10*	Pink-orange	NAg	N/A	11.2 ± 2.2
Δ*bcsA galE*::Tn*10*	Pink	NAg	N/A	10.6 ± 1.1

[a] *S. enteritidis* strains as described in Materials and Methods.
[b] Color of colonies judged after growth on TCR agar for 24 h at 37°C.
[c] The morphology of colonies was compared to that of the 3b parent strain Ag(++), most aggregative (colonies dry and difficult to break apart); Ag(+), aggregative (colonies dry but easier to break apart); NAg, nonaggregative (colonies mucoid).
[d] Colony phenotypes of analogous *S. enterica* serovar Typhimurium strains grown on Luria agar without salt (containing 40 μg of CR per ml and 20 μg of Coomassie brilliant blue per ml) rdar, red, dry, and rough; bdar, brown, dry, and rough; pdar, pink, dry, and rough; saw, smooth and white. Phenotypes are as reported previously (35, 36, 48).
[e] Amount of CR eluted from 10 A_{600} units of cells ± standard error of the mean from four independent experiments.
[f] N/A, not applicable.

color change was observed, and a small increase in CR binding was measured (Table 1). These results confirm that AgfA, AgfB, and subsequent Tafi fibers represent the major CR binding component produced by *S. enterica* serovar Enteritidis 3b (11), while cellulose and LPS O polysaccharide and have relatively minor effects.

Intercellular complementation of Tafi between *S. enterica* serovar Enteritidis 3b Δ*agfB* and Δ*agfA* strains. To effect intercellular formation of Tafi between cells, *S. enterica* serovar Enteritidis Δ*agfA* and Δ*agfB* mutant strains depleted of LPS O polysaccharide (O antigen) or devoid of cellulose were grown closely side by side on TCR agar at 28 or 37°C for 24 or 48 h. No regions of CR binding or other changes in colony color were apparent for any the Δ*agfA* colonies grown beside Δ*agfB* colonies, indicating that Tafi were not being formed between cells. Cross-streaking the different strains together, as recently demonstrated in *E. coli* (9), also did not enable complementation. No colony-associated color changes were seen, indicating that Tafi were not being formed between the cells (data not shown).

To enhance complementation, liquid cultures of each of the four *S. enterica* serovar Enteritidis Δ*agfB* (AgfA donor) and Δ*agfA* (AgfA recipient) strains (Table 1) were mixed and grown together on TCR agar. After 24 h of growth, cells from the 16 different combinations were harvested and the relative CR binding was measured (Fig. 1, upper panels). Significant increases in CR binding were observed for the four combinations in which both donor and recipient strains carried the *galE*::Tn*10* mutation (Fig. 1B and D, last two bars). No significant differences in CR binding were measured in the remaining groups, in which at least one strain was *galE*$^+$ (Fig. 1A and C and Fig. 1B and D, first two bars).

Different levels of CR binding were correlated with cell-associated AgfA detected in the various donor-recipient combinations (Fig. 1, lower panels). Larger amounts of cell-associated AgfA were detected in combinations in which both donor and recipient strains contained *galE*::Tn*10* (Fig. 1B and D, last two lanes). This was in contrast to the other 12 combinations, in which only a trace AgfA band was detectable for the majority of combinations (Fig. 1A and C and Fig. 1B and D, first two lanes). There was some experimental variability, and the levels of cell-associated AgfA did not always correlate with CR binding values (Fig. 1C, compare second and fourth lanes). However, the overall trend indicated that more cell-associated AgfA correlated with increased CR binding. This follows previous findings that increased AgfA polymerization or fimbrial formation correlates with increased levels of CR binding (6, 7, 15, 45).

Characterization of *S. enterica* serovar Enteritidis 3b Δ*agfA* and Δ*agfB* strains and detection of Tafi-associated material. *S. enterica* serovar Enteritidis 3b Δ*agfA* and Δ*agfB* strains (Table 1) were analyzed for the presence of AgfA on Western blots to see if differences existed between the different strains. As expected, AgfA was not detected in any Δ*agfA* strains (Fig. 2A). Cell pellet samples from Δ*agfB* and Δ*agfB* Δ*bcsA* strains were also devoid of AgfA (Fig. 2B, lanes *w*$^+$ and *bcsA*). Unexpectedly, residual cell-associated AgfA was detected in Δ*agfB* strains carrying the *galE*::Tn*10* mutation (Fig. 2, lanes *galE* and *galE bcsA*),. This also correlated with an increase in CR binding in these strains (Table 1).

To test for secretion of AgfA by the Δ*agfB* mutants, cell-free agar plug samples were also analyzed. AgfA was detected in samples corresponding to each of the four *S. enterica* serovar Enteritidis 3b Δ*agfB* strains (Fig. 2B, right panel). Similar amounts of AgfA were detected without formic acid-induced depolymerization, indicating that the AgfA monomers were in an unpolymerized soluble form (data not shown). More AgfA was detected for *galE*::Tn*10* strains (Fig. 2, lanes *galE* and *galE bcsA*), but the difference between strains was small. Thus,

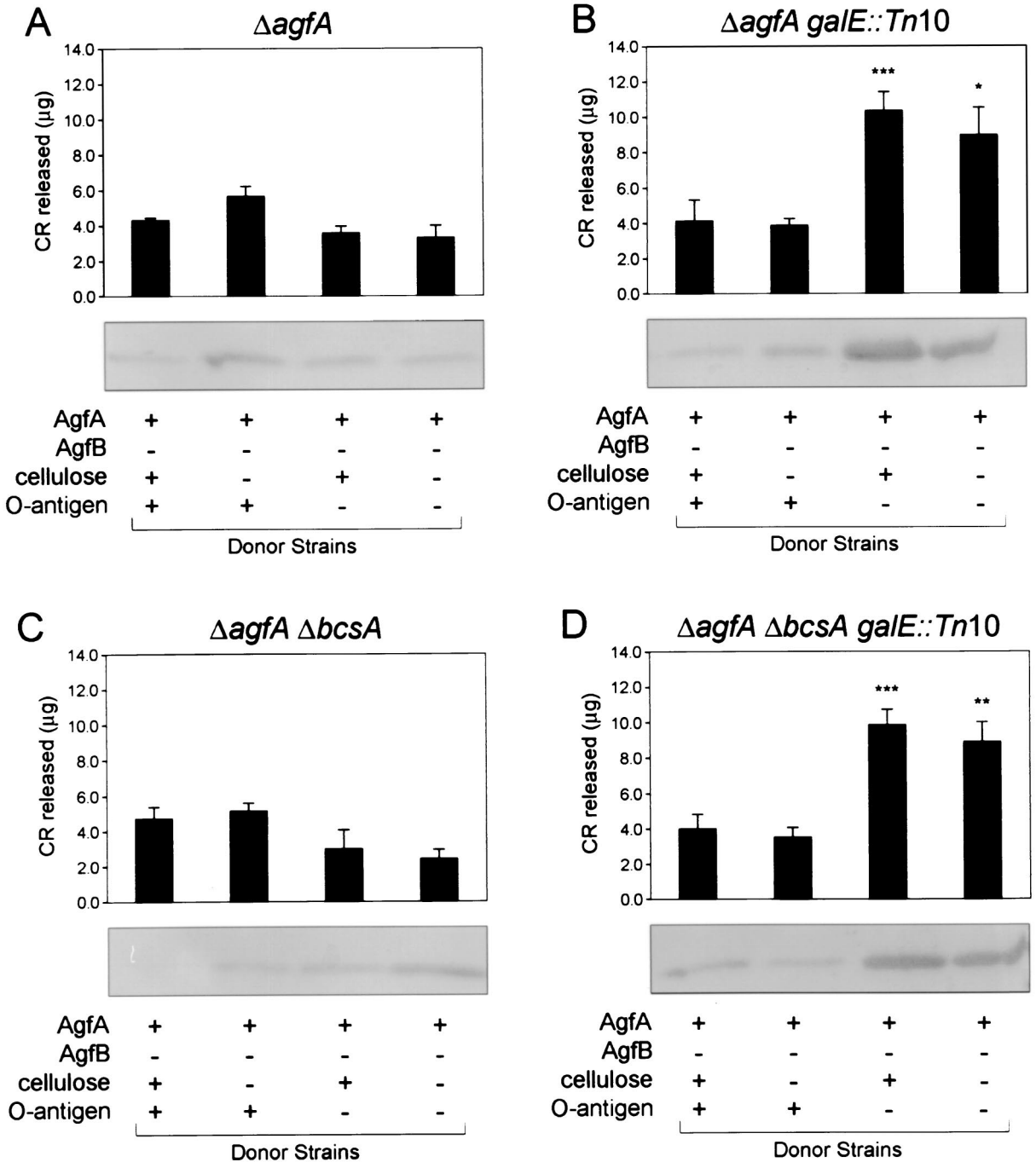

FIG. 1. Intercellular complementation of Tafi between *S. enterica* serovar Enteritidis 3b Δ*agfB* donor and Δ*agfA* recipient strains. CR binding of different Δ*agfA* recipient strains grown together with Δ*agfB* donor strains is shown. Recipient strain genotypes are indicated above each graph, while Δ*agfB* donor strain phenotypes are listed at the bottom. CR binding values for each combination of mutants were normalized by subtracting values for the corresponding Δ*agfB* or Δ*agfA* strains grown individually. Each bar shows the averages and standard errors from four separate experiments, and asterisks indicate significant differences within each group (*, $P < 0.05$; **, $P < 0.01$; ***, $P < 0.001$ [Tukey-Kramer multiple comparisons test]). The panels below the bar graphs show immunoblot analysis performed with immune serum raised to purified Tafi. The amount of AgfA fimbrial material associated with recipient and donor cells scraped off the TCR agar is noted for each recipient-donor combination.

removal of cellulose or O antigen did not have a large effect on secretion of AgfA in the Δ*agfB* strains.

High-molecular-weight (high-MW) immunoreactive material was detected in two of the four Δ*agfA* and Δ*agfB* cell pellet samples (Fig. 2, lanes w^+ and *galE*). In contrast, the high-MW material was not detected in cell pellet samples from Δ*bcsA* strains (Fig. 2, lanes *bcsA* and *galE bcsA*). This indicated that the material was associated with the presence of cellulose. However, pure cellulose was not immunoreactive with Tafi-specific immune serum (data not shown). Therefore, the

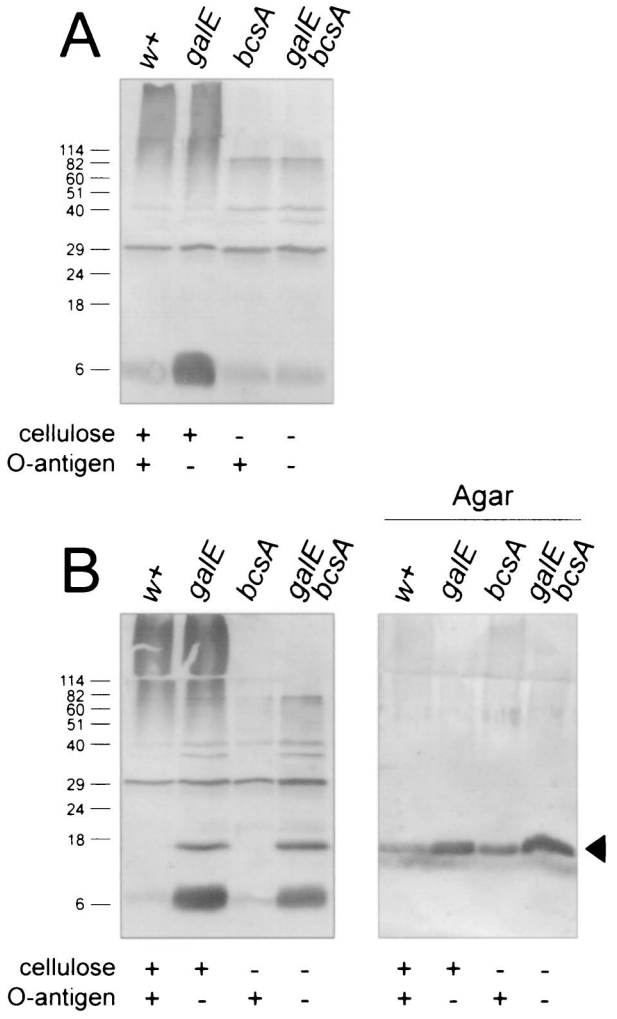

FIG. 2. Western blot analysis of *S. enterica* serovar Enteritidis 3b Δ*agfB* donor and Δ*agfA* recipient strains for the production of AgfA. *S. enterica* serovar Enteritidis 3b Δ*agfA* (A) and Δ*agfB* (B) strains were analyzed for production of AgfA after growth on T agar. Samples from strains were loaded as indicated, and strain phenotypes are listed below each lane. Panel A and the first four lanes of panel B represent proteins in the debris left over after boiling cells in SDS-PAGE sample buffer, whereas agar samples (B) represent proteins present in agar plugs after cells were removed. All samples were treated with formic acid prior to loading on SDS-PAGE. AgfA and associated material were detected by using immune serum raised to purified Tafi; the arrowhead in panel B indicates monomeric AgfA. Molecular mass markers (in kilodaltons) are indicated on the left.

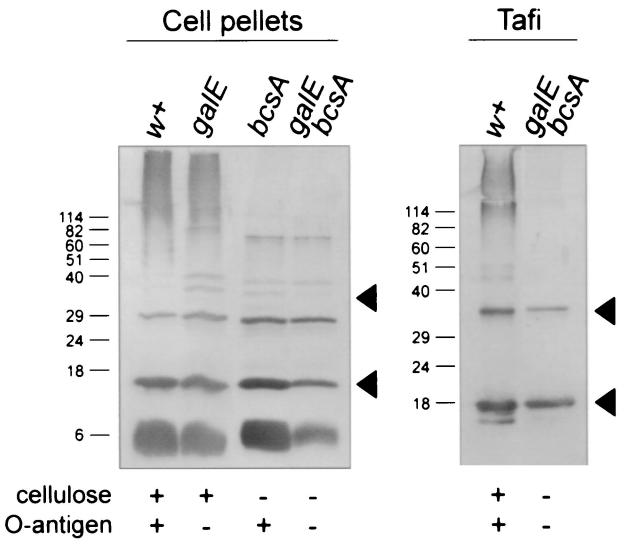

FIG. 3. Immunoblot analysis of AgfA and associated material produced by *S. enterica* serovar Enteritidis 3b and related strains. Proteins in the debris left over after boiling cells in SDS-PAGE sample buffer (cell pellets) or purified fimbrial material (Tafi) from *S. enterica* serovar Enteritidis 3b (w^+) the *galE*::Tn*10* strain (*galE*), the Δ*bcsA* strain (*bcsA*), or the *galE*::Tn*10* Δ*bcsA* strain (*galE bcsA*) were loaded as indicated. Strain phenotypes are listed below each immunoblot. All samples were treated with 90% formic acid prior to loading on SDS-PAGE. AgfA and associated material were detected by using immune serum raised to whole Tafi; the lower and upper arrowheads indicate monomeric and dimeric AgfA, respectively. Molecular mass markers (in kilodaltons) are indicated on the left..

high-MW material was distinct from AgfA, AgfB, and cellulose.

Immunological characterization of *S. enterica* serovar Enteritidis 3b *agfBA*$^+$ strains. To investigate Tafi production by *agfBA*$^+$ *S. enterica* serovar Enteritidis 3b strains (Table 1), cell pellet samples were analyzed for levels of AgfA (Fig. 3). Overall, the levels of AgfA detected in each strain were very similar (Fig. 3, left panel), which correlates with high levels of CR binding for each strain (Table 1). Thus, depleting O polysaccharide or removing cellulose had little or no effect on overall Tafi production within individual cells.

Like for the Δ*agfB* or Δ*agfA* strains, high-MW immunoreactive material was detected in cell pellets from *bcsA*$^+$ strains (Fig. 3, lanes w^+ and *galE*). Again, this immunoreactive material was not found in cell pellets from Δ*bcsA* strains (Fig. 3, lanes *bcsA* and *galE bcsA*). The high-MW material appeared to be tightly cell associated only when cellulose was produced.

To test whether Tafi could be separated from this high-MW material, we purified fimbrial material from *S. enterica* serovar Enteritidis 3b Δ*bcsA galE*::Tn*10* by the procedure outlined by Collinson et al. (12). Western blot analysis of these purified Tafi showed that only AgfA and its associated dimer were detected (Fig. 3, lanes *galE bcsA*) and not the high-MW immunoreactive material; however, it could be seen along with AgfA in Tafi purified from *S. enterica* serovar Enteritidis 3b (Fig. 3, lanes w^+). Therefore, Tafi could be separated from this high-MW material in *S. enterica* serovar Enteritidis 3b, but only when cellulose was not produced,.

Electron microscopy of *S. enterica* serovar Enteritidis 3b and Tafi with or without cellulose. The appearances of Tafi produced by *S. enterica* serovar Enteritidis 3b *bcsA*$^+$ and Δ*bcsA* strains were compared by using electron microscopy (Fig. 4). Immunogold labeling of *S. enterica* serovar Enteritidis 3b cells with an AgfA-specific monoclonal antibody most often showed Tafi as a diffuse fimbrial mat extending from the cell surface (Fig. 4A). Some cells were devoid of labeled fimbrial material, while the majority were intermediate in Tafi production (data not shown). In dramatic contrast, Tafi produced by *S. enterica* serovar Enteritidis 3b Δ*bcsA* were visualized as distinct, curling fibers with precise antibody labeling (Fig. 4B). In general, less fimbrial material was labeled on these cells.

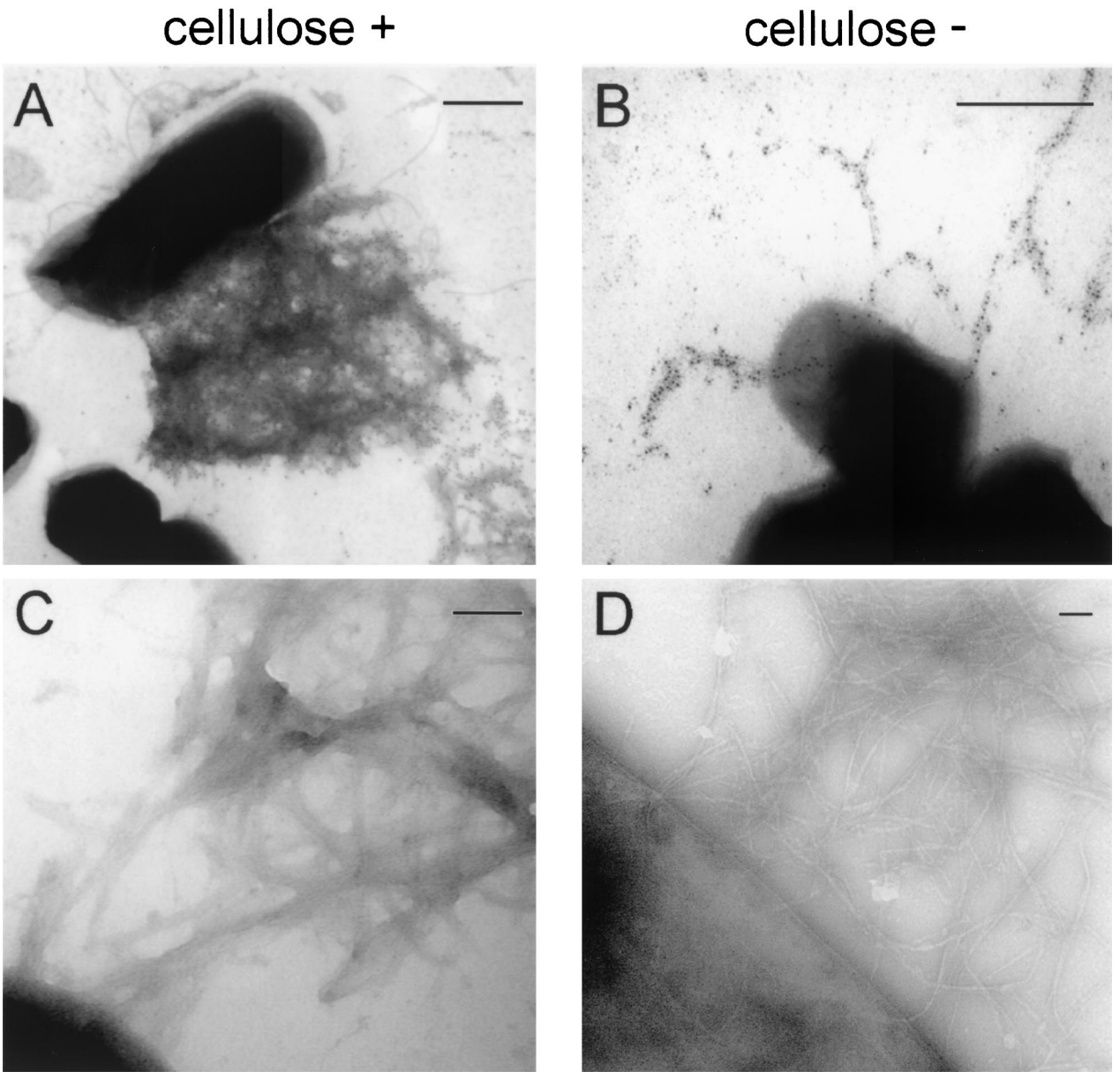

FIG. 4. Transmission electron microscopy of Tafi fimbriae. Fimbriae produced by *S. enterica* serovar Enteritidis strain 3b (cellulose positive) (A and C) or the Δ*bcsA* mutant (cellulose negative) (B and D) were immunogold labeled with AgfA-specific monoclonal antibody 3A-12 ascites followed by goat anti-mouse immunoglobulin–10-nm-diameter gold (A and B) or simply negatively stained with uranyl acetate (C and D). Bars, 500 nm (A and B) or 100 nm (C and D).

For observation of fimbrial material at higher magnifications, cell samples were negatively stained without antibody labeling (Fig. 4C and D). When *S. enterica* serovar Enteritidis 3b Tafi networks were visualized under higher magnifications, no fine detail or individual fibers could be resolved (Fig. 4C). The fimbrial material was quite diffuse. Tafi produced by *S. enterica* serovar Enteritidis 3b Δ*bcsA* were easily resolved into distinct individual fibers (Fig. 4D), although some fibers appeared to be occasionally branched. These observations indicated that *S. enterica* serovar Enteritidis 3b Tafi are closely associated with cellulose at the cell surface.

Detection of Tafi-associated material in *S. enterica* serovar Typhimurium and *E. coli* strains. *S. enterica* serovar Enteritidis 3b, *S. enterica* serovar Typhimurium SL7207, and *E. coli* Vietnam I/1 were tested for production of Tafi and high-MW material after growth at 28 or 37°C (Fig. 5). AgfA (CsgA) was detected in cell pellets from each strain grown at 28°C but was detected only in *S. enterica* serovar Enteritidis 3b and *E. coli* Vietnam I/1 at 37°C (Fig. 5A). CsgA produced by *E. coli* Vietnam I/1 (Fig. 5A) migrated more slowly than AgfA, as reported previously (13).

High-MW immunoreactive material found in the stacking

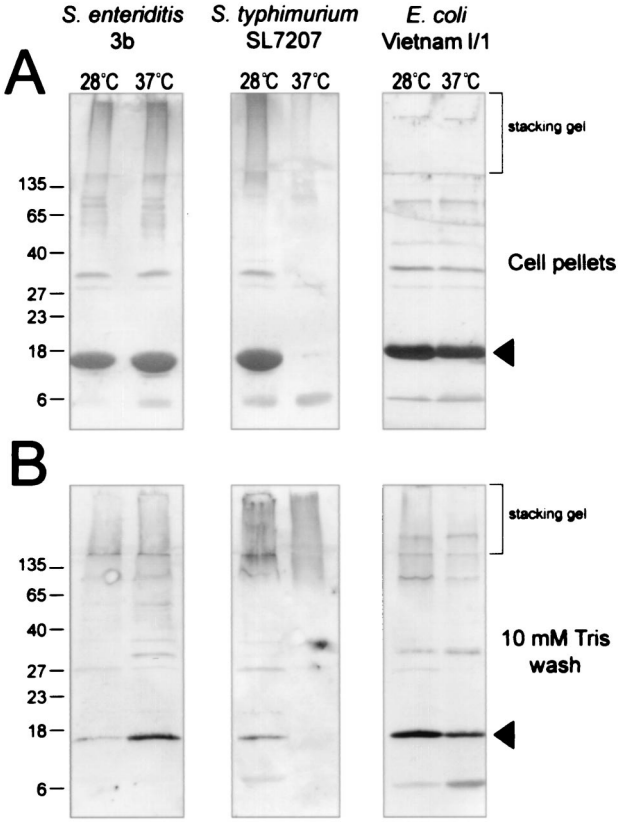

FIG. 5. Detection of immunoreactive Tafi-associated material in different enterobacterial species. Proteins in the debris left over after boiling cells in SDS-PAGE sample buffer (cell pellets) or acetone-precipitated proteins from a 10 mM Tris (pH 8) wash of whole cells of *S. enterica* serovar Enteritidis 3b, *S. enterica* serovar Typhimurium SL7207 or *E. coli* Vietnam I/1 after growth on T agar at 28 or 37°C were loaded as indicated. The brackets show the regions of immunoblots corresponding to the stacking gel from SDS-PAGE. AgfA and associated material were detected by using immune serum raised to whole Tafi; arrowheads indicate monomeric AgfA (*Salmonella*) or CsgA (*E. coli*). Molecular mass markers (in kilodaltons) are indicated on the left.

gel was detected in cell pellet samples from *S. enterica* serovar Enteritidis 3b at 28 and 37°C and in *S. enterica* serovar Typhimurium SL7207 at 28°C (Fig. 5A, first three lanes, stacking gel). The *E. coli* samples were devoid of this material, and only traces were detected for *S. enterica* serovar Typhimurium SL7207 grown at 37°C (Fig. 5A, last three lanes). However, the high-MW material was detected in a pH 8, 10 mM Tris wash of these same cells (Fig. 5B, last three lanes, stacking gel). The material appeared to wash completely off the cells, suggesting that these cells were devoid of cellulose. The high-MW material was also detected in washes of *S. enterica* serovar Enteritidis 3b grown at 28 and 37°C and in washes of *S. enterica* serovar Typhimurium SL7207 grown at 28°C (Fig. 5B, first three lanes), indicating that it was not entirely associated with the cell pellet. However, small amounts of AgfA were detected in these lanes (Fig. 5B), and the material may have been associated with Tafi that washed off. The immunoreactive high-MW material likely represents a substance which is commonly found with Tafi (curli) in *Salmonella* and *E. coli*.

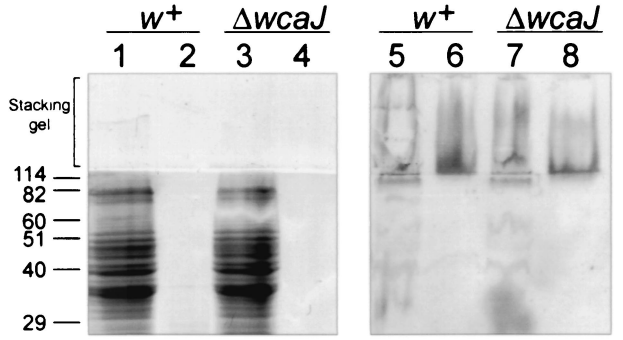

FIG. 6. Detection of high-MW immunoreactive material in *S. enterica* serovar Enteritidis 3b and Δ*wcaJ* strains. SDS-PAGE (lanes 1 to 4) or immunoblot analysis (lanes 5 to 8) of whole cells of the *S. enterica* serovar Enteritidis 3b (w^+) and Δ*wcaJ* strains boiled in SDS-PAGE sample buffer (lanes 1, 3, 5, and 7) and digested with 0.5 mg of proteinase K per ml for 1 h at 65°C (lanes 2, 4, 6, and 8) is shown. Proteins were detected with GelCode staining (Pierce) (lanes 1 to 4). High-MW material was detected by using immune serum raised to purified Tafi (lanes 5 to 8). The bracket shows the stacking gel region of SDS-PAGE and the corresponding immunoblot. Molecular mass markers (in kilodaltons) are indicated on the left.

The high-MW material associated with cellulose and Tafi is a polysaccharide but not CA. CA is an anionic EPS that has been detected in association with curli (Tafi) in *E. coli* (14, 33). Purified CA (25) has a high-MW smearing migration pattern on SDS-PAGE, and its composition is relatively conserved between *S. enterica* serovar Enteritidis, *S. enterica* serovar Typhimurium, and *E. coli* (16, 18). To investigate whether the high-MW material detected by Tafi-specific immune serum represented CA, an isogenic *S. enterica* serovar Enteritidis 3b CA mutant strain (Δ*wcaJ* mutant) was generated. The *wcaJ* gene encodes the initiating undecaprenylphosphate glucose phosphotransferase (41) that is required for CA production in *E. coli* (1).

Immunoreactive high-MW material was detected on Western blots of cell pellet samples from both the 3b parent and Δ*wcaJ* strains (Fig. 6, lanes 5 and 7), indicating that the material did not represent CA. Furthermore, no differences in colony morphology were observed between the Δ*wcaJ* strain and *S. enterica* serovar Enteritidis 3b after growth at 28 or 37°C on TCR agar (data not shown). The high-MW material was resistant to digestion with proteinase K (Fig. 6, lanes 6 and 8) and did not stain with GelCode blue (Fig. 6, lanes 1 to 4), indicating that it was not proteinaceous. Small amounts of purified material tested positive for the presence of uronic acids (data not shown). These data, together with the migration pattern on SDS-PAGE, suggest that the high-MW material represents an uncharacterized anionic polysaccharide that is distinct from CA. This material may be a common component of the Tafi-cellulose extracellular matrix.

DISCUSSION

We discovered that LPS O polysaccharide is the principle factor impeding intercellular Tafi formation in *S. enterica* serovar Enteritidis 3b. Experiments to achieve intercellular formation of Tafi between Δ*agfA* (AgfA recipient) and Δ*agfB*

(AgfA donor) strains of *S. enterica* serovar Enteritidis 3b were repeatedly unsuccessful. Increases in CR binding occurred only when Δ*agfA* and Δ*agfB* strains were grown together and only when both donor and recipient cells carried a *galE*::Tn*10* mutation interfering with LPS O-polysaccharide biosynthesis. Previously we observed that neither AgfA nor AgfB was freely diffusible in *S. enterica* serovar Enteritidis 3b (46), unlike CsgA and CsgB in *E. coli* MC4100 (20). In *E. coli* MC4100, CsgA subunits secreted by Δ*csgB* colonies readily polymerize onto the cell surface of adjacent cells in Δ*csgA* colonies, resulting in an increase in CR binding (20). Consistent with our findings, *E. coli* MC4100 is a K-12 derivative and does not produce LPS O polysaccharide (27).

It is apparent, then, that an intact LPS integument physically precludes access of exogenous AgfA monomers to the nucleating activity of AgfB at the recipient outer membrane surface. When *galE*$^+$ Δ*agfA* recipient cells were used, AgfA subunits secreted from adjacent Δ*agfB* cells were unable to polymerize into intact fimbriae. All Δ*agfB* donor strains were able to secrete extracellular AgfA, although AgfA subunits were somewhat restricted from diffusing away from the Δ*agfB* cell surface when *galE*$^+$ Δ*agfB* donor cells were used, presumably due to the LPS barrier effect, but this barrier appears to be less restrictive toward AgfA exit than toward AgfA entrance. Introduction of the *galE* mutation did not affect fimbrial formation or subsequent CR binding in wild-type *agfBA*$^+$ cells. In addition, all *agfBA*$^+$ strains had aggregation characteristics similar to those of the *S. enterica* serovar Enteritidis 3b parent. These findings seem to question the role of the fimbrial assembly pathway with respect to the significance of intercellular participation in fimbrial assembly with *w*$^+$ cells, colonies, and biofilms. This is particularly evident with *w*$^+$ *S. enterica* serovar Enteritidis 3b, where there is normally no escape of soluble AgfA monomers to adjacent cells and no assembly into intact fimbriae even when AgfA escape is forced via an AgfB deficiency, unless, of course, access is permitted through a disruption in the LPS integument. Thus, the nucleation-precipitation pathway (20) for assembly of these fimbriae would a priori be restricted to operating principally at the immediate cell surface for each *w*$^+$ cell. The data here seem to confirm AgfB-mediated assembly of AgfA monomers at the cell surface. However, this raises the intriguing question as to how Tafi or curli then undergo entropically driven assembly at the distal fimbrial ends, as envisioned in the original model, considerably distant from the LPS integument in the apparent absence of extracellular soluble AgfA monomers.

Interestingly, the presence of cellulose did not interfere with intercellular Tafi formation. This was surprising, since cellulose is produced at the cell surface (34) and forms part of an extracellular matrix with Tafi (39, 48). Although Tafi and cellulose are coregulated under most conditions (39, 48), this could reflect differences in temporal production.

The appearance of Tafi, viewed by electron microscopy, changed drastically when cellulose was not produced. In *S. enterica* serovar Enteritidis 3b (*bcsA*$^+$), Tafi fibers appeared as a tangled amorphous matrix, as reported previously (12, 36). The ultrastructure of the fibers was not discernible at higher magnifications. In comparison, individual Tafi fibers formed by *S. enterica* serovar Enteritidis 3b Δ*bcsA* were easily resolved and had a distinctive curling appearance. At higher magnifications, the ultrastructure was more distinguishable and what appeared to be branch points were observed. These observations help explain other differences between *S. enterica* serovar Enteritidis 3b and *E. coli* MC4100. While *S. enterica* serovar Enteritidis Tafi fibers were unresolved and sometimes linear in appearance (12, 45), *E. coli* curli fibers appeared to be clearly defined with a curling appearance (9, 20). It can be safely assumed that these differences were due to the presence and absence of cellulose, respectively. It was recently demonstrated that *S. enterica* serovar Enteritidis 3b produces cellulose, while *E. coli* MC4100 does not (48). These observations indicate that cellulose forms a very tight association with Tafi in *S. enterica* serovar Enteritidis 3b.

We have detected another component as part of the extracellular matrix formed by Tafi and cellulose in *S. enterica* serovar Enteritidis 3b. This component migrates as a high-MW smear on SDS-PAGE and is recognized by immune serum raised to purified Tafi. In all prior analyses, it was assumed that the immunoreactive high-MW material represented different levels of Tafi depolymerization. In this study, by comparing cellulose-deficient and -sufficient *S. enterica* serovar Enteritidis strains on Western blots, it was apparent that this high-MW material was quite distinct from AgfA, AgfB, and cellulose. However, cellulose was required to tightly link this material to cells. As confirmation of this, purification of Tafi without this material was successful in a Δ*bcsA* strain. Preliminary analysis showed that the high-MW material is not proteinaceous and is slightly anionic. The material does not appear to be CA, since it is still produced in an *S. enterica* serovar Enteritidis Δ*wcaJ* mutant strain.

Cross-reactive high-MW material was also detected in *S. enterica* serovar Enteritidis, *S. enterica* serovar Typhimurium, and *E. coli*. The high-MW material was detected in *S. enterica* serovar Typhimurium SL7207 under conditions in which Tafi and presumably cellulose were not produced. This indicates that production of the unknown material is not regulated by AgfD. However, extracellular polysaccharide production is often induced in the presence of excess carbon when nitrogen or phosphates are limiting (43), conditions in which *agfD* transcription is also up-regulated (17). We hypothesize that the high-MW material represents an uncharacterized EPS that is sometimes produced in association with Tafi and cellulose. Structural characterization to test this hypothesis is in progress.

We have examined the extracellular components associated with Tafi in order to understand the native state of Tafi (curli) found on *Salmonella* and *E. coli* cell surfaces. The genes coding for Tafi (curli) and cellulose are highly conserved between *Salmonella* spp. and *E. coli* and have been detected in most strains tested so far (5, 15, 34, 41, 42). Production of these components is more limited, to between 60 and 70% of strains tested (13, 15, 18, 30, 34, 39). Production of Tafi (curli) and cellulose has not been directly linked to virulence. Highly invasive *E. coli* strains do not appear to produce curli (30, 38), and *csg* genes coding for *E. coli* curli are almost universally disrupted in closely related *Shigella* spp. (38). This suggests there is a selection pressure against Tafi (curli) production during host invasion, especially since the majority of Tafi (curli)-expressing strains produce fimbriae only at temperatures of below 30°C (15, 30, 37). Cellulose-deficient mutants of *S. enterica* serovar Enteritidis showed no difference in viru-

lence in both the BALB/c mouse and 1-day-old chick infection models (39). Again, there is evidence of selective pressure against cellulose production in highly invasive strains (34).

Tafi and curli do not exist alone as protein fibers under normal conditions. In association with cellulose, they are thought to form an important cellular coating associated with biofilm formation and cell-cell attachment (4, 33, 36, 39), which may be analogous to the aggregative physiological state, the Rugose phenotype (2). Production of a more complex matrix consisting of Tafi, cellulose, and EPS would seem to be particularly advantageous for environmental persistence of *Salmonella* spp. and may even aid in survival in the mammalian gut. Cellulose and EPS have been shown to protect cells against acid and heat (29) and chlorine treatment (39) and presumably would prevent desiccation of cells, aid in nutrient trapping, and contribute to buffering (29, 43). Thus, the evidence presented here suggests that Tafi are an integral component of a stable and protective, complex protein-polysaccharide matrix.

ACKNOWLEDGMENTS

We thank Ian Sutherland for the generous gift of purified CA samples from *E. coli* and *Enterobacter cloacae* and for helpful discussions. We also thank R. Beecroft and T. Otto for production of AgfA-specific monoclonal antibodies, J. Halverson and C. Rajotte for excellent technical assistance, and E. E. Ishiguro, C. Whitfield, A. Boraston, and W. Kim for helpful discussions.

Funding for this work was provided by grants to W. W. Kay from the National Sciences and Engineering Research Council and the Canadian Bacterial Diseases Network.

REFERENCES

1. **Aguilar, A., S. Merino, M. M. Nogueras, M. Regue, and J. M. Tomas.** 1999. Two genes from the capsule of *Aeromonas hydrophila* (serogroup O:34) confer serum resistance to *Escherichia coli* K12 strains. Res. Microbiol. **150:**395–402.
2. **Anriany, Y. A., R. M. Weiner, J. A. Johnson, C. E. De Rezende, and S. W. Joseph.** 2001. *Salmonella enterica* serovar Typhimurium DT104 displays a rugose phenotype. Appl. Environ. Microbiol. **67:**4048–4056.
3. **Arnqvist, A., A. Olsen, J. Pfeifer, D. G. Russell, and S. Normark.** 1992. The Crl protein activates cryptic genes for curli formation and fibronectin binding in *Escherichia coli* HB101. Mol. Microbiol. **6:**2443–2452.
4. **Austin, J. W., G. Sanders, W. W. Kay, and S. K. Collinson.** 1998. Thin aggregative fimbriae enhance *Salmonella enteritidis* biofilm formation. FEMS Microbiol. Lett. **162:**295–301.
5. **Baumler, A. J., A. J. Gilde, R. M. Tsolis, A. W. van der Velden, B. M. Ahmer, and F. Heffron.** 1997. Contribution of horizontal gene transfer and deletion events to development of distinctive patterns of fimbrial operons during evolution of *Salmonella* serotypes. J. Bacteriol. **179:**317–322.
6. **Bian, Z., A. Brauner, Y. Li, and S. Normark.** 2000. Expression of and cytokine activation by *Escherichia coli* curli fibers in human sepsis. J. Infect. Dis. **181:**602–612.
7. **Bian, Z., and S. Normark.** 1997. Nucleator function of CsgB for the assembly of adhesive surface organelles in *Escherichia coli.* EMBO J. **16:**5827–5836.
8. **Chan, R. K., D. Botstein, T. Watanabe, and Y. Ogata.** 1972. Specialized transduction of tetracycline resistance by phage P22 in *Salmonella typhimurium.* II. Properties of a high-frequency-transducing lysate. Virology **50:** 883–898.
9. **Chapman, M. R., L. S. Robinson, J. S. Pinkner, R. Roth, J. Heuser, M. Hammar, S. Normark, and S. J. Hultgren.** 2002. Role of *Escherichia coli* curli operons in directing amyloid fiber formation. Science **295:**851–855.
10. **Collinson, S. K., S. C. Clouthier, J. L. Doran, P. A. Banser, and W. W. Kay.** 1996. *Salmonella enteritidis agfBAC* operon encoding thin, aggregative fimbriae. J. Bacteriol. **178:**662–667.
11. **Collinson, S. K., P. C. Doig, J. L. Doran, S. Clouthier, T. J. Trust, and W. W. Kay.** 1993. Thin, aggregative fimbriae mediate binding of *Salmonella enteritidis* to fibronectin. J. Bacteriol. **175:**12–18.
12. **Collinson, S. K., L. Emody, K. H. Muller, T. J. Trust, and W. W. Kay.** 1991. Purification and characterization of thin, aggregative fimbriae from *Salmonella enteritidis.* J. Bacteriol. **173:**4773–4781.
13. **Collinson, S. K., L. Emody, T. J. Trust, and W. W. Kay.** 1992. Thin aggregative fimbriae from diarrheagenic *Escherichia coli.* J. Bacteriol. **174:**4490–4495.
14. **Danese, P. N., L. A. Pratt, and R. Kolter.** 2000. Exopolysaccharide production is required for development of *Escherichia coli* K-12 biofilm architecture. J. Bacteriol. **182:**3593–3596.
15. **Doran, J. L., S. K. Collinson, J. Burian, G. Sarlos, E. C. Todd, C. K. Munro, C. M. Kay, P. A. Banser, P. I. Peterkin, and W. W. Kay.** 1993. DNA-based diagnostic tests for *Salmonella* species targeting *agfA*, the structural gene for thin, aggregative fimbriae. J. Clin. Microbiol. **31:**2263–2273.
16. **Garegg, P. J., B. Lindberg, T. Onn, and I. W. Sutherland.** 1971. Comparative structural studies on the M-antigen from *Salmonella typhimurium*, *Escherichia coli* and *Aerobacter cloacae.* Acta Chem. Scand. **25:**2103–2108.
17. **Gerstel, U., and U. Romling.** 2001. Oxygen tension and nutrient starvation are major signals that regulate *agfD* promoter activity and expression of the multicellular morphotype in *Salmonella typhimurium.* Environ. Microbiol. **3:**638–648.
18. **Grant, W. D., I. W. Sutherland, and J. F. Wilkinson.** 1969. Exopolysaccharide colanic acid and its occurrence in the *Enterobacteriaceae*. J. Bacteriol. **100:**1187–1193.
19. **Hammar, M., A. Arnqvist, Z. Bian, A. Olsen, and S. Normark.** 1995. Expression of two *csg* operons is required for production of fibronectin- and Congo red-binding curli polymers in *Escherichia coli* K-12. Mol. Microbiol. **18:**661–670.
20. **Hammar, M., Z. Bian, and S. Normark.** 1996. Nucleator-dependent intercellular assembly of adhesive curli organelles in *Escherichia coli.* Proc. Natl. Acad. Sci. USA **93:**6562–6566.
21. **Hashimoto-Gotoh, T., F. C. Franklin, A. Nordheim, and K. N. Timmis.** 1981. Specific-purpose plasmid cloning vectors. I. Low copy number, temperature-sensitive, mobilization-defective pSC101-derived containment vectors. Gene **16:**227–235.
22. **Hoiseth, S. K., and B. A. Stocker.** 1981. Aromatic-dependent *Salmonella typhimurium* are non-virulent and effective as live vaccines. Nature **291:**238–239.
23. **Hone, D., R. Morona, S. Attridge, and J. Hackett.** 1987. Construction of defined *galE* mutants of *Salmonella* for use as vaccines. J. Infect. Dis. **156:** 167–174.
24. **Jackson, D. W., K. Suzuki, L. Oakford, J. W. Simecka, M. E. Hart, and T. Romeo.** 2002. Biofilm formation and dispersal under the influence of the global regulator CsrA of *Escherichia coli.* J. Bacteriol. **184:**290–301.
25. **Junkins, A. D., and M. P. Doyle.** 1992. Demonstration of exopolysaccharide production by enterohemorrhagic *Escherichia coli.* Curr. Microbiol. **25:**9–17.
26. **Laemmli, U. K.** 1970. Cleavage of structural proteins during the assembly of the head of bacteriophage T4. Nature **227:**680–685.
27. **Liu, D., and P. R. Reeves.** 1994. *Escherichia coli* K12 regains its O antigen. Microbiology **140:**49–57.
28. **Loferer, H., M. Hammar, and S. Normark.** 1997. Availability of the fibre subunit CsgA and the nucleator protein CsgB during assembly of fibronectin-binding curli is limited by the intracellular concentration of the novel lipoprotein CsgG. Mol. Microbiol. **26:**11–23.
29. **Mao, Y., M. P. Doyle, and J. Chen.** 2001. Insertion mutagenesis of *wca* reduces acid and heat tolerance of enterohemorrhagic *Escherichia coli* O157: H7. J. Bacteriol. **183:**3811–3815.
30. **Olsen, A., A. Arnqvist, M. Hammar, S. Sukupolvi, and S. Normark.** 1993. The RpoS sigma factor relieves H-NS-mediated transcriptional repression of *csgA*, the subunit gene of fibronectin-binding curli in *Escherichia coli.* Mol. Microbiol. **7:**523–536.
31. **Olsen, A., H. Herwald, M. Wikstrom, K. Persson, E. Mattsson, and L. Bjorck.** 2002. Identification of two protein-binding and functional regions of curli, a surface organelle and virulence determinant of *Escherichia coli.* J. Biol. Chem. **277:**34568–34572.
32. **Prigent-Combaret, C., E. Brombacher, O. Vidal, A. Ambert, P. Lejeune, P. Landini, and C. Dorel.** 2001. Complex regulatory network controls initial adhesion and biofilm formation in *Escherichia coli* via regulation of the *csgD* gene. J. Bacteriol. **183:**7213–7223.
33. **Prigent-Combaret, C., G. Prensier, T. T. Le Thi, O. Vidal, P. Lejeune, and C. Dorel.** 2000. Developmental pathway for biofilm formation in curli-producing *Escherichia coli* strains: role of flagella, curli and colanic acid. Environ. Microbiol. **2:**450–464.
34. **Romling, U.** 2002. Molecular biology of cellulose production in bacteria. Res. Microbiol. **153:**205–212.
35. **Romling, U., Z. Bian, M. Hammar, W. D. Sierralta, and S. Normark.** 1998. Curli fibers are highly conserved between *Salmonella typhimurium* and *Escherichia coli* with respect to operon structure and regulation. J. Bacteriol. **180:**722–731.
36. **Romling, U., M. Rohde, A. Olsen, S. Normark, and J. Reinkoster.** 2000. AgfD, the checkpoint of multicellular and aggregative behaviour in *Salmonella typhimurium* regulates at least two independent pathways. Mol. Microbiol. **36:**10–23.
37. **Romling, U., W. D. Sierralta, K. Eriksson, and S. Normark.** 1998. Multicellular and aggregative behaviour of *Salmonella typhimurium* strains is controlled by mutations in the *agfD* promoter. Mol. Microbiol. **28:**249–264.
38. **Sakellaris, H., N. K. Hannink, K. Rajakumar, D. Bulach, M. Hunt, C. Sasakawa, and B. Adler.** 2000. Curli loci of *Shigella* spp. Infect. Immun. **68:**3780–3783.

39. **Solano, C., B. Garcia, J. Valle, C. Berasain, J. M. Ghigo, C. Gamazo, and I. Lasa.** 2002. Genetic analysis of *Salmonella enteritidis* biofilm formation: critical role of cellulose. Mol. Microbiol. **43:**793–808.
40. **Soto, G. E., and S. J. Hultgren.** 1999. Bacterial adhesins: common themes and variations in architecture and assembly. J. Bacteriol. **181:**1059–1071.
41. **Stevenson, G., K. Andrianopoulos, M. Hobbs, and P. R. Reeves.** 1996. Organization of the *Escherichia coli* K-12 gene cluster responsible for production of the extracellular polysaccharide colanic acid. J. Bacteriol. **178:**4885–4893.
42. **Stevenson, G., R. Lan, and P. R. Reeves.** 2000. The colanic acid gene cluster of *Salmonella enterica* has a complex history. FEMS Microbiol. Lett. **191:** 11–16.
43. **Sutherland, I.** 2001. Biofilm exopolysaccharides: a strong and sticky framework. Microbiology **147:**3–9.
44. **Uhlich, G. A., J. E. Keen, and R. O. Elder.** 2001. Mutations in the *csgD* promoter associated with variations in curli expression in certain strains of *Escherichia coli* O157:H7. Appl. Environ. Microbiol. **67:**2367–2370.
45. **White, A. P., S. K. Collinson, P. A. Banser, D. J. Dolhaine, and W. W. Kay.** 2000. *Salmonella enteritidis* fimbriae displaying a heterologous epitope reveal a uniquely flexible structure and assembly mechanism. J. Mol. Biol. **296:**361–372.
46. **White, A. P., S. K. Collinson, P. A. Banser, D. L. Gibson, M. Paetzel, N. C. Strynadka, and W. W. Kay.** 2001. Structure and characterization of AgfB from *Salmonella enteritidis* thin aggregative fimbriae. J. Mol. Biol. **311:**735–749.
47. **White, A. P., S. K. Collinson, J. Burian, S. C. Clouthier, P. A. Banser, and W. W. Kay.** 1999. High efficiency gene replacement in *Salmonella enteritidis*: chimeric fimbrins containing a T-cell epitope from *Leishmania major.* Vaccine **17:**2150–2161.
48. **Zogaj, X., M. Nimtz, M. Rohde, W. Bokranz, and U. Romling.** 2001. The multicellular morphotypes of *Salmonella typhimurium* and *Escherichia coli* produce cellulose as the second component of the extracellular matrix. Mol. Microbiol. **39:**1452–1463.